ORIGINAL RESEARCH ARTICLE

Validation and statistical analysis of the Group for High Resolution Sea Surface Temperature data in the Arabian Gulf

Oleksandr Nesterov [a],[*], Marouane Temimi [b], Ricardo Fonseca [c], Narendra Reddy Nelli [c], Yacine Addad [a], Emmanuel Bosc [d], Rachid Abida [a]

[a] Department of Nuclear Engineering, Emirates Nuclear Technology Center, Khalifa University of Science and Technology, UAE
[b] Department of Civil, Environmental, and Ocean Engineering (CEOE), Stevens Institute of Technology, Hoboken, NJ, USA
[c] ENGEOS Lab, Research Division, Khalifa University of Science and Technology, UAE
[d] Federal Authority for Nuclear Regulation, Abu Dhabi, UAE

Abstract The combined effect of climate change and steadily increasing seawater demand for industrial and domestic purposes in the Arabian Gulf region has a significant impact on the ecosystem in this region. Additionally, this effect may reduce the efficiency and increase the operating costs of industrial facilities that utilize seawater for cooling and other purposes. In this context, it is important to know various statistical characteristics of the sea surface temperature (SST) and their trends, in addition to the mean climatological characteristics. The analysis conducted in this study utilized a 17-year Group for High Resolution Sea Surface Temperature Level 4 dataset of $0.01 \times 0.01°$ spatial resolution. First, the dataset was compared against a 2-year seawater temperature measurements at the ten offshore buoys in the relatively shallow coastal waters of the United Arab Emirates between Ras Ghumais and Dubai, which showed a reasonably good agreement between the two datasets, with the estimated root mean square deviations ranging from 0.5 to 0.9°C. Subsequently, several statistical SST characteristics were calculated. The trend analysis showed not only positive tendencies in the mean SSTs of up to 0.08°C/year in the northern Gulf, but also the trends in the annual percentile exceedances, particularly the 95th percentiles (near-maximum SSTs), which increased

---

* Corresponding author at: Department of Nuclear Engineering, Emirates Nuclear Technology Center, Khalifa University of Science and Technology, P.O. Box: 127788, UAE.
  E-mail address: oleksandr.nesterov@ku.ac.ae (O. Nesterov).

by approximately 0.07°C/year in the western United Arab Emirates and eastern Qatar waters. On the contrary, the 5th percentiles (near-minimum SSTs) decreased by up to 0.1°C/year, especially in the waters around Bahrain, Qatar, and the western United Arab Emirates. These results indicate that extreme hot and cold SST events in the Gulf are becoming more frequent and more extreme than before.

1. Introduction

The Arabian Gulf, hereinafter called the Gulf, is a relatively shallow semi-enclosed water body connected to the Sea of Oman through the Strait of Hormuz (Figure 1). It is located in a hot, arid environment and subjected to high natural water temperatures reaching 36°C in summer (Chandy et al., 1990; Dubach, 1964; Reynolds, 1993). Such high temperatures not only pose significant risks to the natural ecosystem, particularly causing coral reef bleaching (Aeby et al., 2020; Claereboudt, 2009) and the extinction of some seagrass and fish species (Sheppard et al., 2010), but also they may adversely impact the efficiency of industrial facilities utilizing seawater for cooling, such as power generation and petrochemical processing plants.

The discharge of heated effluents from large industrial facilities, such as those in Ruwais, United Arab Emirates (UAE) (Elshorbagy et al., 2013; Nesterov et al., 2010), intensify these risks. To mitigate the negative environmental impacts of heated effluents, regulatory authorities in many Gulf Cooperation Council countries imposed thresholds on heated effluent temperatures, primarily via allowable increments above the background levels. For example, in the UAE, the excess effluent temperature must be less than 5°C at the discharge point, and the allowable difference from the background sea surface temperature (SST) must be within ±3°C (ERWDA, 1999). In Saudi Arabia, the excess effluent temperature must not exceed 10°C at the discharge point, the maximum increase must be less than 2.2°C, and the monthly average increase must be less than 2°C (Royal Commission for Jubail and Yanbu, 2004). In Qatar, the cooling water temperature difference must not exceed 3°C at the discharge point (Supreme Council for the Environment and Natural Reserves, 2002). In the Sultanate of Oman, the weekly average increases must not exceed 1°C outside a 300 m radius zone (Ministry of Regional Municipalities, 2005). However, these regulations do not include provisions to mitigate the extremely hot temperatures in summer, which is a highly important aspect to cooling water system designers and operators, and marine ecologists (e.g., Aeby et al., 2020), especially taking into consideration the trends in air temperature extremes (Al Sarmi and Washington, 2014). Furthermore, the natural variability of ambient conditions, climate change (Chowdhury and Al-Zahrani, 2013), and interferences of effluents from various industrial facilities in coastal areas complicate and make the definition of background water temperatures ambiguous. As a result, this may potentially lead to the formation of relatively hot water pockets near outfalls, where temperatures may approach or even exceed 40°C in summer. Technically, this condition may still be compliant with the formal regulations despite causing severely negative environmental impacts, such as coral bleaching (Aeby et al., 2020) and deterioration of water quality, which are expected to be dependent on the persistence time of these conditions and their frequency of re-occurrence.

A thorough understanding of the statistical characteristics of seawater temperatures in the Gulf is critical to the design of various cooling water facilities, estimating their efficiencies and potential downtime caused by extreme water temperature events, providing more detailed quantitative information to marine ecologists, and establishing a foundation for future improvements in regulations. Percentile exceedances (a percentile indicates the temperature value, below which a specified percentage of the samples in a set of samples falls) appear suitable for such a characterization, along with the time exceedances (a percentage of the time SSTs exceed a specified temperature value). In contrast to the conventional mean climatological characteristics that have been extensively reported in the publicly available literature, there is a lack of studies dedicated to the analysis of these characteristics.

Compared to in situ measurements, such as those by Mezhoud et al. (2016), satellite SST data collected over several decades are suitable for estimating long-term trends, particularly in remote offshore and inaccessible areas. Pastor et al. (2018) utilized a long-term high-resolution dataset provided by the Group for High-Resolution Sea Surface Temperature (GHRSST) to determine SST trends in the Mediterranean Sea. GHRSST data was also utilized by Reul et al. (2014) to study the movement of the Gulf Stream in the Atlantic Ocean. Noori et al. (2019) used the relatively coarse 0.25°-resolution NOAA Daily Optimum Interpolation SST Anomaly satellite dataset from 1982 through 2015 to determine the mean SST trends in the Gulf and Sea of Oman, and also estimate the minimum and maximum SST. However, these aforementioned studies did not report statistical quantities, such as percentile exceedances, which are as important as the seasonal mean characteristics. The 5th (P_{05}) and 95th (P_{95}) percentiles are often considered good approximations of the minimum and maximum, respectively. They are more reliable and less noisy quantities compared to the exact maximum and minimum over a study period, and less prone to instrumentation, processing, and other errors. Detailed exceedance statistics could be useful in assessing efficiencies of cooling water facilities and determining the possibility of downtimes; hence, they are often utilized in feasibility and front-end engineering design studies (e.g., Bath et al., 2004).
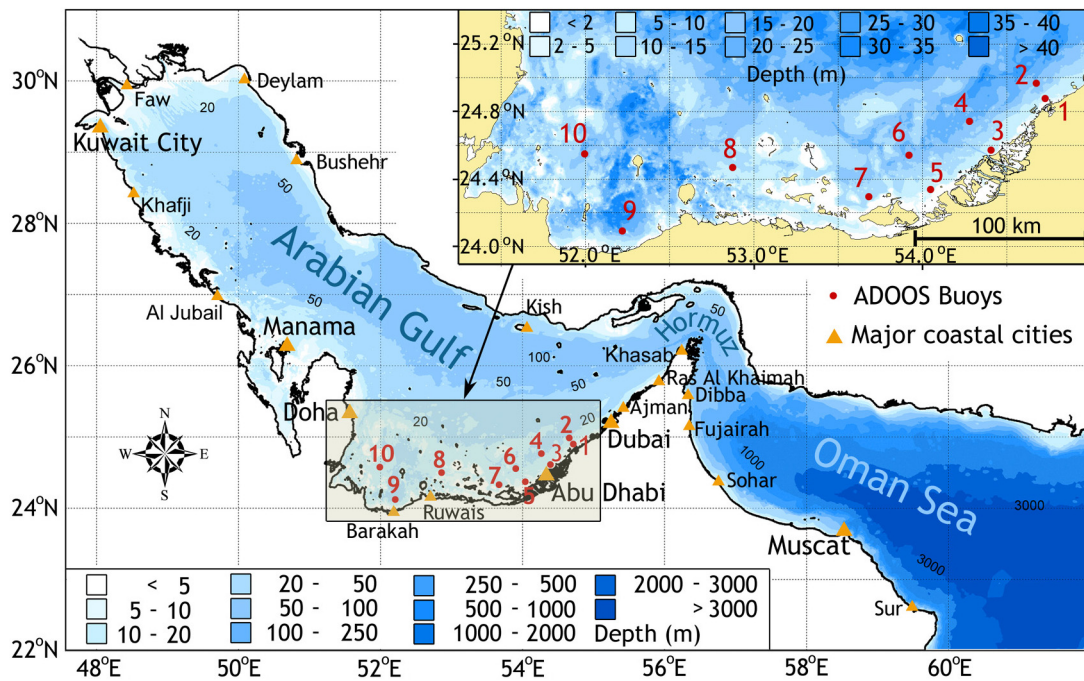
Figure 1 Spatial extent of the study area, bathymetry (with respect to admiralty chart datum), locations of the ten ADOOS buoys, and selected coastal sites.

The availability of continuous high-resolution data products has led to the rapidly increased number of studies on the long-term trends of various parameters derived from satellite optical sensors, including studies in the Arabian Gulf, in the recent decade. Al-Rashidi et al. (2009) analyzed 18 years of SST data obtained via the Advanced Very High Resolution Radiometer (AVHRR) satellite and estimated an annual trend of 0.05 ± 0.03°C/year in the northern Gulf. Utilizing SSTs from the NOAA Extended Reconstructed SST version 3 dataset, Shirvani et al. (2015) determined trends of 0.003—0.04 and 0.0005—0.05°C/year in the southern and northern Gulf, respectively. According to Noori et al. (2019), the mean trend was approximately 0.03°C/year. The GHRSST Level 4 dataset used in this study has a significantly higher spatial resolution of 0.01° × 0.01°, which is beneficial for coastal zones and constricted areas, particularly shallow areas in the western UAE and near Qatar, where most depths are less than 40 m, and along the northwestern shores of the Gulf near river mouths, where a large spatiotemporal SST variability is expected. For instance, the existence of the local SST decrease in the Strait of Hormuz near Khasab, which is discussed later in this study, may also be found in the June-, July-, and August-averaged SSTs plots presented in Moradi and Kabiri (2015); however, there is no evidence of this decrease in relatively coarse 0.25°-resolution data analyzed by Noori et al. (2019).

For the analysis of trends, an alternative to long-term observation data would be numerical modeling. However, numerical grids utilized in most modeling studies of the circulation in the Gulf were of relatively coarse resolution compared to the spatial resolution of GHRSST Level 4 dataset, or only covered local problem-specific areas (e.g., Al Azhar et al., 2016; Azam et al., 2006; Elshorbagy et al., 2006; Kämpf and Sadrinasab, 2006; Pous et al., 2015). Note-

worthy, accurate calibration of the parameterizations of surface fluxes in numerical models and high-quality meteorological forcing data are essential to accurately reproduce the SSTs, on which these fluxes, particularly the latent heat flux, depend on. A relatively recent study by Elhakeem et al. (2015), which focused on a long-term simulation of the Gulf hydrodynamics, concluded that water evaporation in the Gulf is primarily controlled by meteorological forcing (i.e., humidity, air temperature, cloud cover, and wind) and warm water inflow from the Sea of Oman through the Strait of Hormuz in winter. Xue et al. (2015) simulated future conditions in the Gulf using a coupled atmosphere—ocean model and estimated annual surface evaporation in the Gulf of 1.84 m/year, consistent with that of Reynolds (1993). These studies emphasized the important role of SST in heat and water exchanges with the atmosphere. The numerical modeling is better suited for studying three-dimensional fields and estimating derived quantities such as heat fluxes. In contrast, remote sensing data are often preferable for analyzing quantities at the sea surface, in part because of the avoidance of complex parameterizations of physical processes, inaccuracies in numerical approximations of differential equations, and uncertainties in external forcing. Moreover, remote sensing data can be utilized for validation of numerical models.

Noteworthy, the microphysics of the top few centimeters of the water layer, particularly the high attenuation of the infrared spectrum of solar radiation and evaporation-related processes, leads to a non-trivial definition of SST. The Group for High Resolution SST distinguishes the interface, skin (defined as the temperature measured by an infrared radiometer typically operating at 3.7—12 μ wavelengths), sub-skin, and foundation SSTs (Minnett and Kaiser-Weiss, 2012), with typical differ-

ences of a few degrees Celsius between them. Foundation SST is more suitable for climatological studies and comparison with numerical simulations because its temporal variability occurs relatively slowly compared to the diurnal variabilities of the interface, skin, and sub-skin SSTs. Despite these complexities in defining the foundation SSTs and uncertainties in the remotely sensed skin SSTs due to the presence of dust in arid and semi-arid regions (e.g., Bogdanoff et al., 2015), a high-resolution satellite-based data product is preferable to analyze SST variability and trends in the Arabian Gulf, taking into consideration all the uncertainties and limitations of numerical modeling.

The relatively high spatial resolution of the GHRSST Level 4 data product of $0.01° \times 0.01°$ compared to other publicly available datasets, combined with the availability of data since 2002, allows this dataset to be used in many applications, such as validation of regional circulation models, setting up open boundary conditions for local hydrodynamics models, and statistical analyses. In connection with these potential applications, the three main objectives of this study are as follows:

1. Assessment of the GHRSST Level 4 dataset accuracy against 2-year in situ temperature data obtained from the sensors installed on the ten offshore buoys, which are deployed in the UAE coastal waters as a component of the Abu Dhabi Ocean Observing System (ADOOS).
2. The calculation of percentiles and time exceedances describing SST variability in the Gulf, supplemented by discussions on the observed features and their links with local atmospheric and hydrodynamic processes.
3. The estimations of the trends in the climatological mean SSTs, and inter-annual trends in annual 5th and 95th percentile SSTs.

The spatial extent of the study domain was selected as to cover typical regions of the numerical simulations of the circulations in the Gulf and Sea of Oman (e.g., Al Azhar et al., 2016; Elhakeem et al., 2015; Elshorbagy et al., 2006; Kämpf and Sadrinasab, 2006; Nesterov et al., 2010; Pous et al., 2015).

The overall methodology and datasets employed in this study are described in Section 2. The accuracy of the GHRSST Level 4 dataset is evaluated against the in situ ADOOS buoy measurement data followed by a detailed statistical analysis of the seasonal and annual variabilities, particularly the trends of the mean, 5th and 95th percentile SSTs, in Section 3. The main findings of the analysis and suggested future studies are summarized in Section 4. Wind fields, which are used to support discussions, and tabulated statistical information extracted at several economically important coastal locations are included in Appendix A.

2. Material and methods

The high-level overview of the overall methodology and a detailed description of all the datasets utilized in this study are presented below.

2.1. Methodology

The overall methodology of this study was as follows. Firstly, the two-dimensional gridded fields of daily $0.01° \times 0.01°$-resolution GHRSST Level 4 data corresponding to the foundation SST were acquired for the study domain from 2003 through 2019. Notably, the satellite data products covering longer intervals of time, such as the AVHRR satellite data analyzed in Noori et al. (2019), are also publicly available; however, these datasets have significantly lower spatial resolutions, typically ranging from 0.25 to 0.05°. After that, daily SST time series were extracted from the gridded GHRSST dataset at the ten locations closest to the respective geographical locations of the ADOOS buoys and then visually compared with the available in situ ADOOS data over the 2017−2018 period. The visual comparison was supplemented by the estimation of the root mean square differences (RMSD) and correlation coefficients between the daily averaged ADOOS data and the time series extracted from GHRSST (the original ADOOS temperature records were of 10-min temporal resolution). Additionally, the in situ temperature data were used to statistically characterize the diurnal SST cycle, including deviations from daily averages. This helps to better understands differences that could naturally be expected between in situ measurements and satellite-derived data products.

The two-dimensional fields were computed after that for the four types of statistics:

1. Conventional climatological means.
2. Fifth (P_{05}), 25th (P_{25}), 75th (P_{75}), and 95th (P_{95}) percentile SSTs.
3. Time exceedances of 24, 27, 30, and 33°C defined as the percentages of samples exceeding these specified SST levels.
4. The long-term trends in the mean SSTs, and the trends in annual 5th and 95th percentile SSTs, accompanied by a p-value test to determine statistical significance.

The conducted statistical analysis is supplemented by discussions and associations with the meteorological and hydrodynamic processes in the Gulf area, aimed at explaining the observed SST features. Detailed descriptions of the datasets utilized in this study are provided below. Hereinafter, in the frame of this study the term SST conventionally implies foundation SST, and the term GHRSST denotes the GHRSST Level 4 dataset, unless stated otherwise.

2.2. Observational and reanalysis datasets

The four observational datasets utilized in this study include the daily GHRSST dataset of $0.01° \times 0.01°$ spatial resolution, the in situ SST records obtained from ten ADOOS offshore marine buoys, the in situ weather observation data in Barakah (UAE), and the ERA-5 reanalysis dataset (Hersbach et al., 2020).

The GHRSST is an international group that includes satellite data providers, which deliver data to the Data Assembly Center (http://ghrsst.jpl.nasa.gov), and eventually makes this product available for reanalysis and online distribution (http://ghrsst.nodc.noaa.gov). The GHRSST Level 4 data

are obtained by the blending and optimal interpolation of data from various sources, including the AVHRR satellite, Moderate Resolution Imaging Spectroradiometer (MODIS), WindSAT Remote Sensing System, and the in situ SST Quality Monitor (iQUAM) operated by the National Oceanographic and Atmospheric Administration (NOAA), and the National Environmental Satellite, Data, and Information Service (NESDIS). Further information about the GHRSST data product can be found, for example, in Banzon et al. (2016). The utilized GHRSST data are representative of the foundation SST defined at 10 m depth (Minnett and Kaiser-Weiss, 2012). Although the GHRSST data is available from June 2002, the analyzed interval was selected as to span over the integer number of years (from 2003 through 2019) to eliminate the effects of seasonality on the statistical quantities. Noteworthy, the raw satellite data subsets used to produce GHRSST Level 4 dataset could have higher or lower spatial resolution than the final product. Due to this reason, the effects of spatiotemporal interpolation are occasionally evident in the individual daily GHRSST fields.

The ten ADOOS buoy locations are indicated in Figure 1. These buoys were deployed in the UAE waters, covering approximately 320 km of alongshore coastal stretches between Ras Ghumais and Dubai. They have been maintained by the Marine Information Section, Spatial Data Division of the Department of Municipalities and Transport of the Abu Dhabi City Municipality since 2015. The SST records, which were made available for this study, cover the 2017—2018 period at the temporal resolution of 10 min. The sensors installed at the buoys measure oceanographic, meteorological, and water quality parameters. The XYLEM-YSI EXO conductivity and temperature sensor, engineered for compatibility with EXO2′s central wiper system (a multi-parameter water quality monitoring platform; https://www.ysi.com/products/multiparameter-sondes), was used for seawater temperature measurements. This instrument can operate in a temperature range from −5 to 50°C with an accuracy of 0.2°C. Relatively weak currents, such as those observed at Buoy No. 9 off the Barakah coast in western UAE, where the current speed averaged over 2017—2018 was only 5 cm/s in the water of approximately 20 m depth (with respect to admiralty chart datum), suggest a dominant influence of the meteorological forcing on the SST. This makes ADOOS data highly suitable for the analysis of the SST diurnal cycles.

An analysis of relevant meteorological fields was conducted to explain several notable peculiarities in the SST statistics in the study area. The air temperature data were obtained from a meteorological station installed on a tower in Barakah, UAE, approximately 15 km from Buoy No. 9 at the 10 m height above ground level. This air temperature record, which spanned over 2012—2019 at 10-min intervals, was correlated with the measured SSTs at Buoy No. 9 to explain an approximate one-month lag in the timings of the annual maximum SST occurrences in the Gulf compared to those in the Sea of Oman.

Additionally, ERA-5 wind and air temperature reanalysis data (Hersbach et al., 2020) were used to support the proposed explanations of several SST peculiarities in the Gulf. ERA-5 is the latest reanalysis product developed by the European Centre for Medium-Range Weather Forecast. ERA-5 meteorological fields are available at a 0.25° × 0.25° spatial resolution starting from 1979. ERA-5 has been found to outperform other reanalysis datasets in a wide range of applications, such as hydrological studies in India (Mahto and Mishra, 2019) and the simulation of the solar radiation in western Pakistan (Tahir et al., 2020).

3. Results

The high resolution of GHRSST data can particularly be useful to visualize surface currents and fine-scale flow structures. For example, in addition to heat exchange with the atmosphere and vertical mixing, the horizontal heat transport in the Sea of Oman is influenced by large mesoscale eddies (e.g., Pous et al., 2004, 2015; Reynolds, 1993) driven by general circulation in the Arabian Sea (Qasim, 1982), which subsequently cascade into many smaller sub-mesoscale eddies. These smaller eddies and their remnants are occasionally traceable in individual daily GHRSST fields (Figure 2), especially along the southern coast between Sohar and Dibba, being consistent with the reported results of numerical modeling (e.g. Pous et al., 2015). The existence of these eddies was previously confirmed by drifters (e.g., Reynolds, 1993) and measured current transects (Pous et al., 2004). Reynolds (1993) also reported the upwelling zone at the Iranian coast (Figure 2), resultant from the confluence of two mesoscale eddies, but no strong evidence of its existence in that area was found in the analyzed GHRSST data.

Various numerical simulations (e.g., Al Azhar et al., 2016; Kämpf and Sadrinasab, 2006) supported by Reynolds (1993) expedition data have demonstrated a general counterclockwise circulation in the Arabian Gulf, which is also observed in the GHRSST data, for example, such as in the daily snapshots depicted in Figure 2. The surface water from the Sea of Oman, which enters the Gulf through the Strait of Hormuz (Swift and Bower, 2003), flows northwest along the Iranian coast causing a moderating effect on the SSTs in the central Gulf. Occasionally in winter, this surface current in conjunction with periodic tidal motion forms a vortex street noticeable in GHRSST plots (Figure 2). In contrast, the SSTs in the northern Gulf are primarily governed by heat exchange with the atmosphere, especially during Shamal wind events (strong northwesterly winds). Several studies, which included estimations of the surface heat fluxes and heat transport through the Strait of Hormuz, have been performed in the past (e.g., Ahmad and Sultan, 1990; Elhakeem et al., 2015; Pous et al., 2015; Xue and Eltahir, 2015). The SSTs in the upper northwestern Gulf are also notably affected by freshwater river inflows from Iran and Iraq.

The southern part of the Gulf between the UAE and eastern Qatar, which is called southern shallows (Kämpf and Sadrinasab, 2006), is known for its highest water temperatures within the Gulf region during summer. The currents in this area, where depths are generally less than 40 m, are significantly affected by the abundance of islands, shallow tidal flats, and the relatively narrow passages between them. Also, it features the highest measured salinities in the Gulf (up to 46 psu at Ruwais; Azam et al., 2006). The currents in the southern shallows may vary in a wide range depending on a location. For example, at Buoy No. 9 (location is indicated in Figure 1), stagnant conditions were
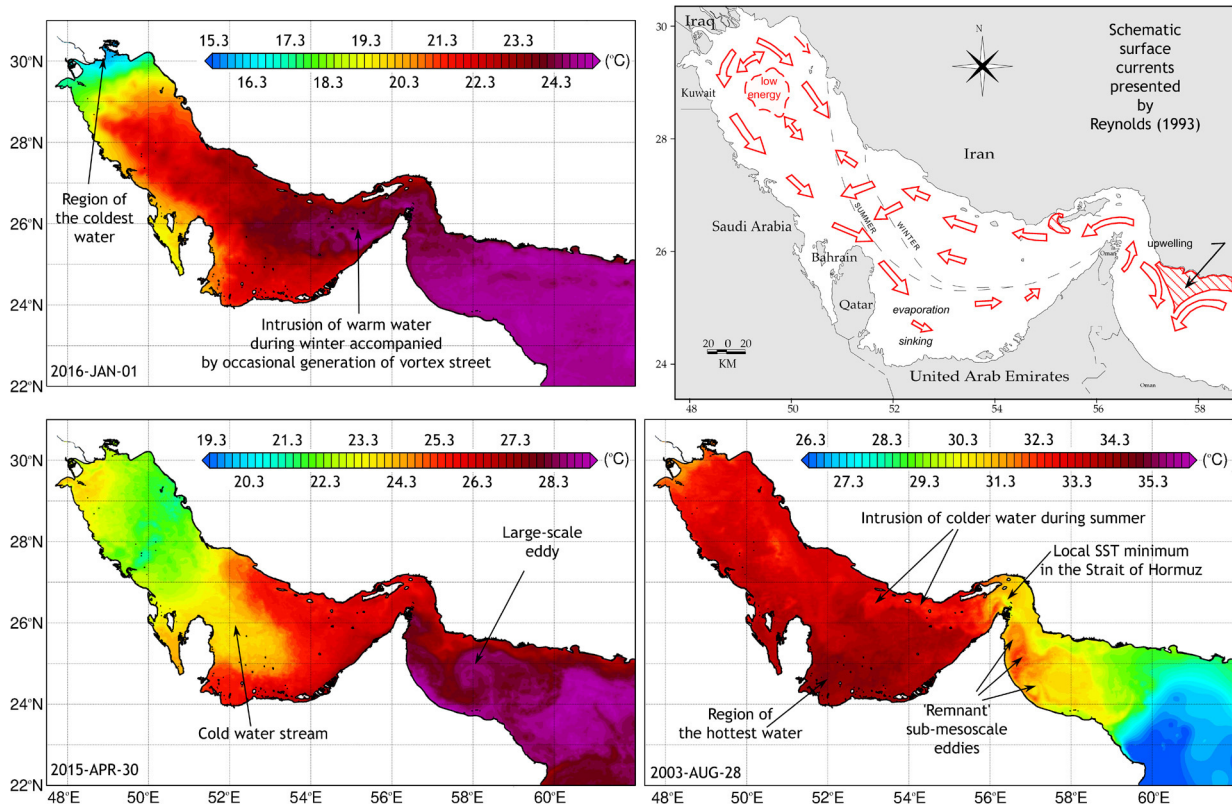
Figure 2 Schematic surface currents in the Arabian Gulf after Reynolds (1993), and fine-scale flow features traceable in several daily GHRSST data snapshots.

observed during the entire 2017−2018 period, with the current speed exceeding 0.15 m/s in less than 5% of the time and the average being of approximately 0.05 m/s. In contrast, relatively strong currents were observed at Buoy No. 8, where current speeds occasionally reached 1 m/s. As a result, the vertical mixing, which consequently affects the SST, can be expected to significantly vary across the southern shallows.

Before performing a statistical analysis of the two-dimensional GHRSST data, it is important to conduct assessment of its accuracy in the Gulf region, which was achieved by comparing it with the in situ temperature records as detailed in Section 3.1, and investigate inherent discrepancies due to the different natures of the GHRSST and in situ data, particularly with regard to what temperatures these datasets represent.

3.1. Comparison of GHRSST data with in situ measurements

A visual comparison of the ADOOS buoy water temperature time series with the GHRSST data extracted at corresponding locations is presented in Figure 3. The extraction was performed at the GHRSST grid points nearest the respective buoy locations. Interpolation was not deemed necessary due to the high 0.01° × 0.01° spatial resolution of the GHRSST dataset.

The GHRSST data represent foundation SSTs at 10 m depth, which have a practically negligible response to the diurnal skin or subskin SST fluctuations (Minnett and Kaiser-Weiss, 2012). In contrast, the ADOOS buoy SSTs were recorded close to the water surface, and they clearly exhibited diurnal variability, thus leading to inherent differences compared to the foundation SSTs, which were larger during summer as expected. Despite the different natures of ADOOS and GHRSST datasets, the daily averaged buoy data were found to be in a reasonably good agreement, particularly during the autumn and winter seasons, when the mixed layer deepened.

To remove the diurnal variability before conducting statistical comparison with the GHRSST data, the ADOOS buoy temperature data were averaged daily. The resultant scatter plots are shown in Figure 4, and the detailed tabulated seasonal statistics are presented in Table A1 in the Appendix. As seen, GHRSST data are in a good agreement with in situ SSTs, with the RMSDs being in the range from 0.54°C to 0.86°C for the different locations.

It is worth noting that the root mean square errors (RMSE; note the difference between RMSD and RMSE definitions in the frame of this study: the former is associated with the differences between GHRSST and ADOOS data; the latter is an auxiliary field included in GHRSST datasets) extracted from the GHRSST datasets at the ADOOS buoy locations and then averaged over the 2017−2018 period, are found in the range from 0.37 to 0.39°C. The larger RMSDs estimated in this study compared to RMSEs included in the GHRSST dataset are likely because the comparison was conducted without adjusting the ADOOS buoy temperatures to the foundation SST. Furthermore, according to Bogdanoff et al. (2015), the error in SST data retrievals associated with aerosols can be as high as 1°C, which may indicate the necessity of respective adjustments of GHRSST data
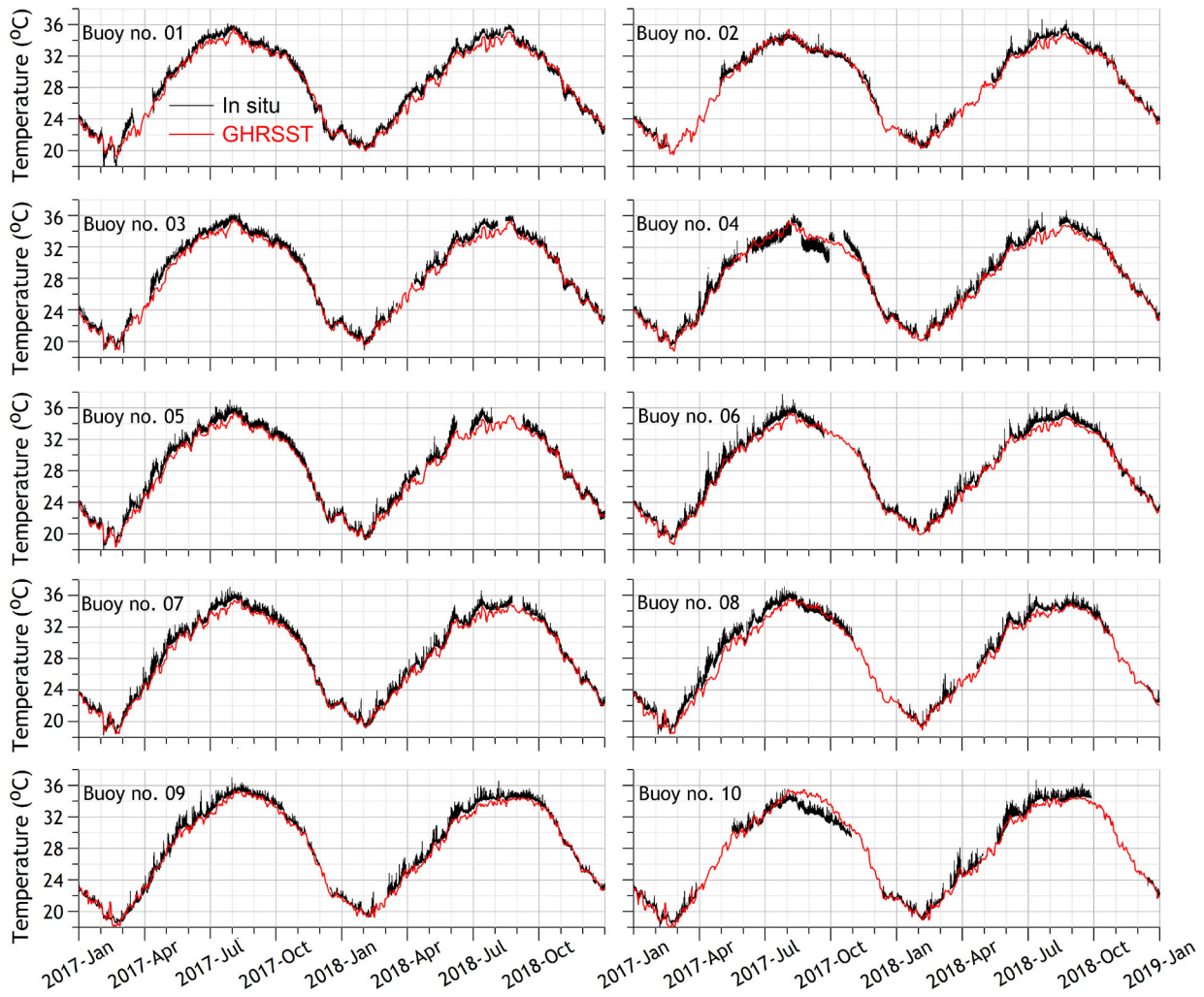
Figure 3 Visual comparison of the 2017—2018 ADOOS buoy and GHRSST data at the corresponding buoy locations.
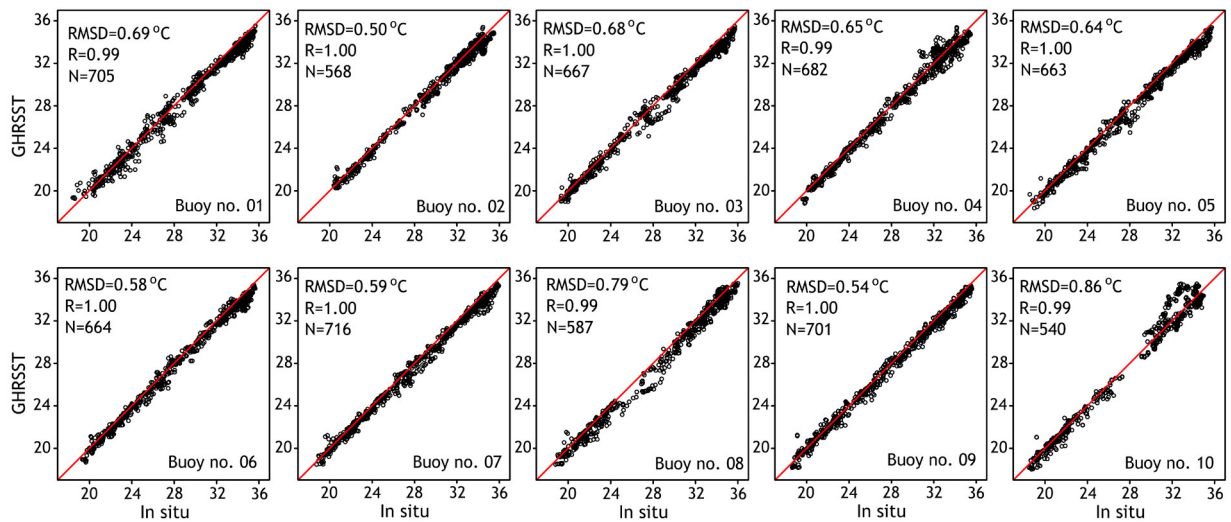

Figure 4 Comparison of the daily-averaged ADOOS buoy and GHRSST data at the ten buoy locations. The root mean square difference (RMSD), correlation coefficient (*R*), and the number of samples compared (*N*) are indicated at the top left of each panel.
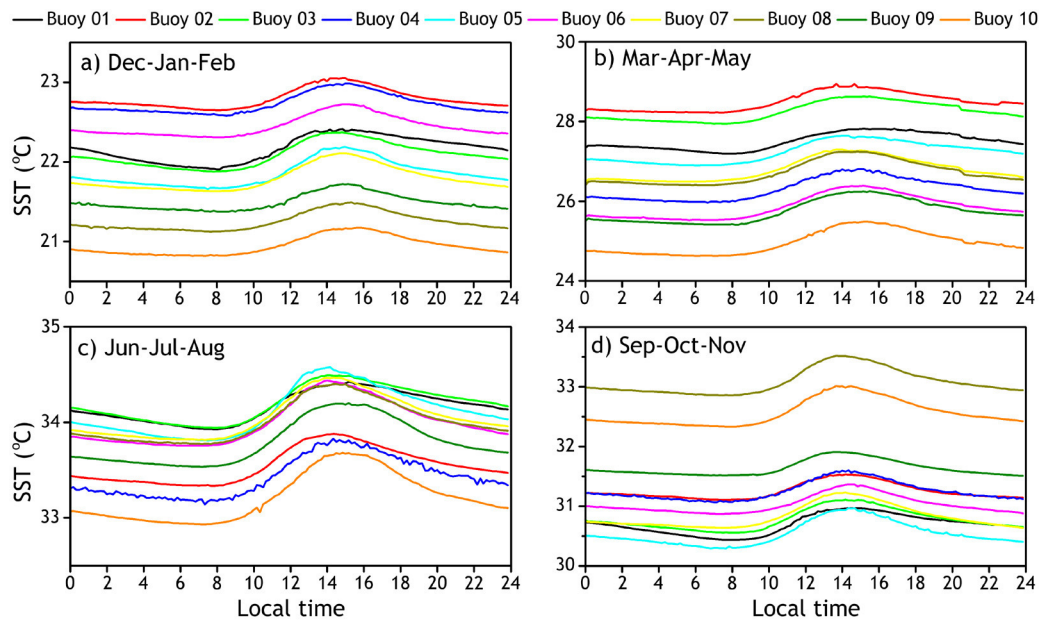
Figure 5 Diurnal cycles of the SSTs derived from the ADOOS buoys data, averaged over the (a) DJF, (b) MAM, (c) JJA and (d) SON seasons.

in the Gulf region for further improvements. Therefore, the RMSDs estimated in this study are within the expected magnitude of fluctuation due to various factors, such as local weather effects, diurnal variability, and the physics of heat transfer in the near-surface and skin layers.

A further analysis of the scatter plots (Figure 4) revealed the weak dependence of the RMSDs on the number of samples, with the highest RMSD occurring at Buoy No. 10 due to the availability of only 540 samples. In addition to the good agreement of magnitudes, both the datasets exhibited similar phases, with correlation coefficients exceeding 0.99. Therefore, it can be concluded that the GHRSST dataset is suitable for statistical analysis, with expected mean errors of up to 1°C in the Arabian Gulf along the UAE shore.

Interestingly, in the December-January-February (DJF) season, the SSTs generally increased from west to east in the Gulf waters along the UAE coast, with the lowest season-averaged SSTs observed at ADOOS Buoy No. 10 on the far west side and the highest SSTs observed at Buoys Nos. 1 and 2 near Dubai (locations are indicated in Figure 1). This positive west—east gradient is also noted in the GHRSST data (Section 3.3) in DJF and March-April-May (MAM) seasons, while this gradient was smaller in the June-July-August (JJA) and September-October-November (SON) seasons. This is likely due to stronger northwesterly winds in the winter season, as demonstrated in Figure A.1, which presents the monthly mean horizontal winds at 10 m height sourced from ERA-5 data over the 2003—2019 period. Season-averaged temperatures at the buoy locations were in the approximate ranges 21—23°C and 33—35°C in the DJF and JJA seasons, respectively, consistent with those previously reported in the literature (e.g., Xue et al., 2015).

The relatively high temporal resolution of the ADOOS buoy data allowed for an analysis of the diurnal cycles of the SST along the UAE shore, and their evolution throughout the year, which are presented in Figure 5 and supplemented

by a more detailed statistical analysis. To avoid discontinuities, 10-min deviations with respect to the daily means were defined as the differences between an original temperature sample and the running average over a 24-h interval centered at the time the sample was obtained. After that, the series of diurnal extremes of these deviations were extracted for each buoy, yielding up to 730 samples per a set. The gaps in ADOOS data, as well as monotonic changes of the SST over periods longer than 24 hours resulted in lesser numbers of the extracted peaks. The maxima and minima were analyzed separately. The statistics for deviations of the minima were computed as the statistics for absolute deviations and then negated. The computed in this way 25th (P_{25}), 50th (P_{50}; median), 75th (P_{75}), 95th (P_{95}), and 99th (P_{99}) percentiles of the diurnal maxima and minima are presented in Table 1. These results were supplemented by the 25th (P_{25}), 50th (P_{50}), 75th (P_{75}), 95th (P_{95}), and 99th (P_{99}) percentiles of the diurnal variability magnitude, defined as the differences between daily maximum and minimum SSTs at a location. The average and median diurnal deviations from the 24-h running averages were mostly between 0.5 and 1°C, also consistent with those previously reported (e.g., Paparella et al., 2019). However, occasionally these deviations exceeded 3°C in the western UAE waters.

It is interesting to note a spatial increase in the diurnal variability magnitudes from east (near Dubai) to west (Barakah), which was evident in all the derived statistics, especially pronounced in the P_{95} and P_{99} percentiles. Presumably, this effect may be attributed to the weaker sea and land breeze circulations in the western part of the UAE (Eager et al., 2008), which could have resulted in weaker vertical mixing of a water column and/or less intense evaporation. No other correlations that could explain this effect, such as with depth, current, or intensity of solar radiation, were identified in the course of this study.

504

Table 1   Percentile deviations of the daily minimum and maximum with respect to the daily means and diurnal range percentiles at the ten ADOOS buoy locations.

| Buoy no.	Deviations of daily minimum (negated magnitudes, °C)					Deviations of daily maximum (°C)					Diurnal range (°C)				
	P_{25}	P_{50}	P_{75}	P_{95}	P_{99}	P_{25}	P_{50}	P_{75}	P_{95}	P_{99}	P_{25}	P_{50}	P_{75}	P_{95}	P_{99}
01	-0.23	-0.33	-0.44	-0.71	-1.00	0.24	0.36	0.52	0.84	1.08	0.51	0.68	0.93	1.35	1.79
02	-0.16	-0.25	-0.36	-0.57	-0.85	0.24	0.36	0.54	0.93	1.65	0.43	0.61	0.85	1.44	2.14
03	-0.21	-0.31	-0.42	-0.60	-0.87	0.24	0.41	0.60	0.97	1.33	0.54	0.72	0.94	1.48	1.97
04	-0.17	-0.32	-0.55	-0.82	-1.08	0.28	0.49	0.76	1.21	1.98	0.47	0.82	1.34	1.85	2.73
05	-0.25	-0.34	-0.48	-0.70	-0.87	0.34	0.50	0.71	1.19	1.60	0.62	0.86	1.13	1.86	2.38
06	-0.16	-0.26	-0.39	-0.70	-0.95	0.26	0.44	0.72	1.42	2.12	0.42	0.70	1.09	2.00	2.95
07	-0.19	-0.29	-0.42	-0.65	-0.80	0.32	0.46	0.69	1.24	1.74	0.53	0.75	1.10	1.91	2.56
08	-0.20	-0.32	-0.46	-0.69	-0.90	0.28	0.45	0.71	1.29	2.06	0.50	0.76	1.16	1.90	2.84
09	-0.14	-0.24	-0.38	-0.72	-0.90	0.23	0.38	0.66	1.28	2.03	0.38	0.63	1.01	1.96	2.65
10	-0.18	-0.28	-0.41	-0.74	-0.97	0.25	0.47	0.80	1.40	1.85	0.46	0.77	1.17	2.04	3.31
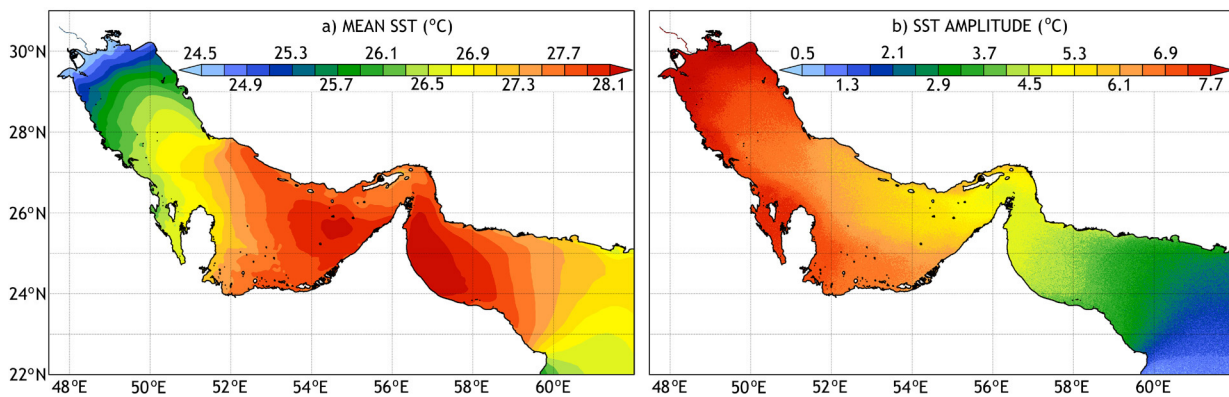
Figure 6   (a) Annual mean SST and (b) SST amplitude.

The unavailability of sub-hourly long-term SST data in other regions of the Gulf and Sea of Oman precludes an analysis of the diurnal SST cycles in other areas of the Gulf and Sea of Oman. Therefore, subsequent discussions focus on statistical characteristics of the SST, including long-term trends, basing on GHRSST data.

3.2. Annual variability

To characterize the annual cycle of SSTs $T_i = T_i(t)$ at every discrete grid point i within the study area, where $t \in [0, 365]$ is the day of a year, it was assumed that the annual cycles averaged over the 2003-2019 period could be approximated by sinusoidal functions in the following form:

$$T_i = M_i + A_i \sin\left(\frac{2\pi}{365}t - \varphi_i\right) \tag{1}$$

where the annual mean SST M_i, the amplitude A_i, and the phase φ_i are individual fitting parameters for every discrete grid point i. The two-dimensional fields of M_i and A_i, which were obtained by the method of least squares, are shown in Figure 6.

The highest annual mean SSTs in the Gulf were estimated at 28°C based on the analyzed GHRSST data, and they were found approximately 80 km northwest of Dubai. Even slightly higher annual mean SSTs of 28.2°C were noted

in the Sea of Oman between Fujairah and Sohar (locations are indicated in Figure 1). The lowest mean SSTs occurred in the northern Gulf, likely due to four main factors. The first factor is the cold air temperatures during the winter (e.g., Al Senafi and Anis, 2015). The second factor is relatively shallow water depths, mostly between 0 and 20 m (Figure 1), resulting in a relatively small heat capacity of the water column. The third factor is the long distance from the Strait of Hormuz, through which relatively warm water from the Sea of Oman penetrates the Gulf during winter (Elhakeem et al., 2015). The fourth factor is the cold freshwater inflows from several rivers.

An interesting peculiarity is that the mean SSTs were approximately 1°C lower in the Strait of Hormuz near Khasab than in the adjacent areas of the Gulf and Sea of Oman. This localized decrease can also be noticed in June-, July-, and August-averaged plots, which were presented by Moradi and Kabiri (2015) based on MODIS data. There are several possible explanations for this effect, such as: local weather effects due to the mountainous shores surrounding the Strait of Hormuz; intense mixing of the water column caused by stronger currents; the surfacing of deeper waters due to the steep bathymetry gradients; local inaccuracies in the GHRSST and MODIS data. Monthly mean wind fields were analyzed to explore the first suggested reason. As seen in Figure A.1 of the Appendix, a localized maximum in the

southeasterly wind speeds between the extreme northeastern tip of the UAE and the adjacent Iranian coast occurred in July and August and gradually weakened in September and October. This leads to several possible consequences: the wind pushes slightly colder water from the Sea of Oman into the Strait of Hormuz along the Iranian coast; the wind increases evaporation rate; the relatively cold air leads to more intense cooling of the water surface. Furthermore, the pattern of weaker winds between Fujairah and Sohar during summer correlates with the pattern of higher SSTs. This peculiarity is also evident in Table A2, which shows that the annual mean SSTs in the coastal region near Fujairah and Sohar are 0.3 to 0.4°C higher than those near Muscat (to the south) and Dibba (to the north). This difference is even larger in the medians (P_{50}), which are 0.4−0.6°C higher in this area than that in the adjacent regions. An analysis of the two other proposed explanations was beyond the scope of this study, particularly because they require the application of an appropriate three-dimensional hydrodynamic model and/or long-term field measurements.

Generally, the SSTs over the Gulf experienced an approximate 5−8°C amplitudes of the annual variability with respect to the annual means, with the largest and smallest observed amplitudes occurring in the northwestern part and the Strait of Hormuz, respectively. This northwest−southeast gradient is due to the larger air temperature variability in the northern Gulf (e.g., Al Senafi et al., 2015) and the intrusion of warmer waters through the Strait of Hormuz (Elhakeem et al., 2015) in winter. In the Sea of Oman, the amplitude of the annual cycle gradually decreases from 5°C in the approaches to the Strait of Hormuz to below 1°C on its southeastern side. This spatial pattern is consistent with that previously reported (e.g., Xue et al., 2015), and it can be attributed to the transition from subtropical weather conditions to a tropical environment. In addition, this effect is exaggerated by the mountain ranges in Oman and Yemen along the coasts, which obstruct propagation of the relatively hot air from the Arabian Peninsula deserts into the basins of the Oman and Arabian Seas. Also, the exchanges with the relatively deep Arabian Sea and the Indian Ocean (e.g., the North Equatorial and Somali currents) and the relatively high heat capacity of the water column due to greater depths contribute to the lower annual variability of the SSTs on the southeastern side of the Sea of Oman.

The timings of the maximum and minimum SST occurrences on average during the 2003−2019 period, are presented in Figure 7a. They were derived from the phases φ_i of sinusoidal fits, and hence the time interval between the occurrences of the maximum and minimum was half a year for all the locations. An interesting peculiarity is that the SST peaks occurred in the offshore Gulf 2−4 weeks later than in the Sea of Oman, except in the near-shore areas of the UAE, Qatar, Saudi Arabia, and Kuwait, where the SSTs mainly reached annual maximum in early to mid-August. This one-month lag is also evident in the timings of the occurrence of the maximum air temperatures at a 2 m height derived from the ERA-5 reanalysis data shown in Figure 7b. This lag can be explained by Figure 7c, which depicts the annual air temperature cycle at the height of 10 m based on the meteorological measurements at the tower in Barakah compared against the annual cycle of the SSTs at Buoy No. 9, located approximately 15 km away from it. As seen, the timing of

the maximum SST occurrences approximately coincide with the timing when the daily mean air temperature and the SST become equal, which is then followed by the period of cooling of both the water and air. Because the air remains warmer than the water surface, the SSTs continue to raise in the Gulf until late August, in contrast to the SSTs in the Sea of Oman. In the shallow coastal areas of the Gulf, the SSTs, however, reach annual maxima faster likely due to the smaller heat capacity of the water column.

3.3. Seasonal variability

The seasonal mean SSTs in the study domain derived from the GHRSST data are shown in Figure 8. In the winter (DJF) and spring (MAM) seasons, the SSTs exhibited a clear west−east temperature gradient. A gradual increase from approximately 16°C north of Kuwait to 25°C in the Sea of Oman is noted in the DJF-averaged SSTs. In the summer (JJA) and autumn (SON) seasons, the SST gradient was reversed, which was expected because the weather conditions are typically more quiescent in the Gulf, as shown in Figure A.1, with the hottest subtropical weather conditions prevailing in the extreme northwestern part of the basin. Furthermore, the northern part of the Gulf is mostly shallow (Figure 1), which results in a faster SST response to changes in meteorological conditions. The highest SSTs were observed in the coastal waters of the western UAE and eastern Qatar during the summer (JJA) season, partly due to the shallowness of this area. In the autumn (SON) season, the peak SSTs shifted offshore, approximately 130 km east of Doha and 130 km north of Ruwais. This feature can presumably be explained by the combination of several factors, which include higher humidity over the water surface that reduces the rate of radiative cooling (i.e., the blanket effect) and deeper water compared to the depths in the southern shallows, which implies a larger heat capacity of the water column and a slower cooling rate as a result.

3.4. Percentile exceedances

The information about percentile exceedances can be more important for certain types of engineering problems and biological studies than the information about climatological means. In particular, the 5th and 95th percentiles, which are typically close to the minimum and maximum, respectively, can be important characteristics to support the design of cooling water facilities to ensure uninterrupted operation during extreme events, and also in environmental impact assessment studies. As noted in the Introduction, these statistical quantities are more reliable than the simple minimum and maximum. The calculated 5th (P_{05}), 25th (P_{25}), 75th (P_{75}), and 95th (P_{95}) percentile SSTs are presented in Figure 9. Being close to the winter lows, the P_{05} statistics (Figure 9a) resemble the DJF-averaged SST (see Figure 8a). The SSTs along the northernmost shores of the Gulf were below 14°C in 5% of the analyzed period 2003−2019. Similarly, the P_{95} statistics (Figure 9d) resemble the JJA-averaged SSTs (see Figure 8c). The SSTs exceeded 33°C in most areas of the Gulf and 34°C in the western UAE and eastern Qatar waters in 5% of the analyzed period. The plots of P_{25} and P_{75} resemble the MAM- and SON-averaged SSTs, respectively. The
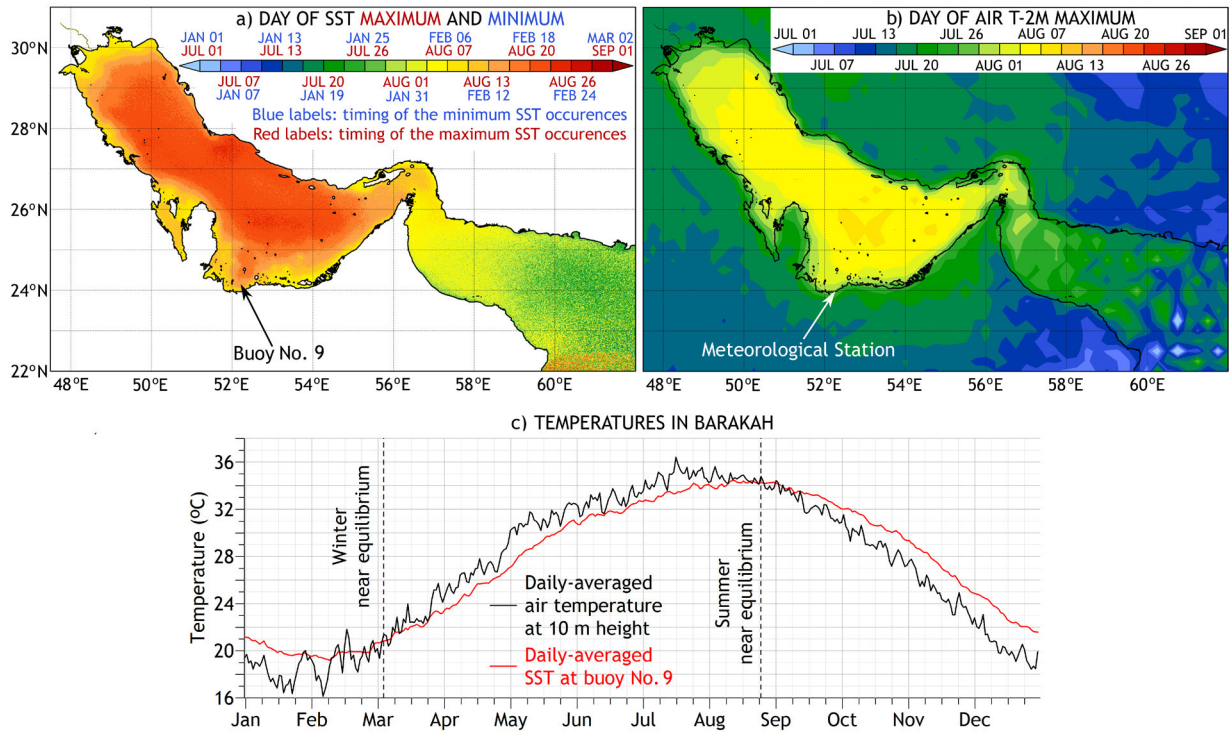
Figure 7 (a) Average timing of the minimum and maximum SST occurrences based on the GHRSST 2003—2019 data; (b) the average day of the occurrence of the peak air temperature at the height of 2 m derived from ERA-5 2003—2019 data; (c) annual cycle of the air temperature measured at a meteorological tower in Barakah, averaged over 2012—2019 period, and the daily SSTs measured at the location of Buoy No. 9, averaged over 2017—2018.
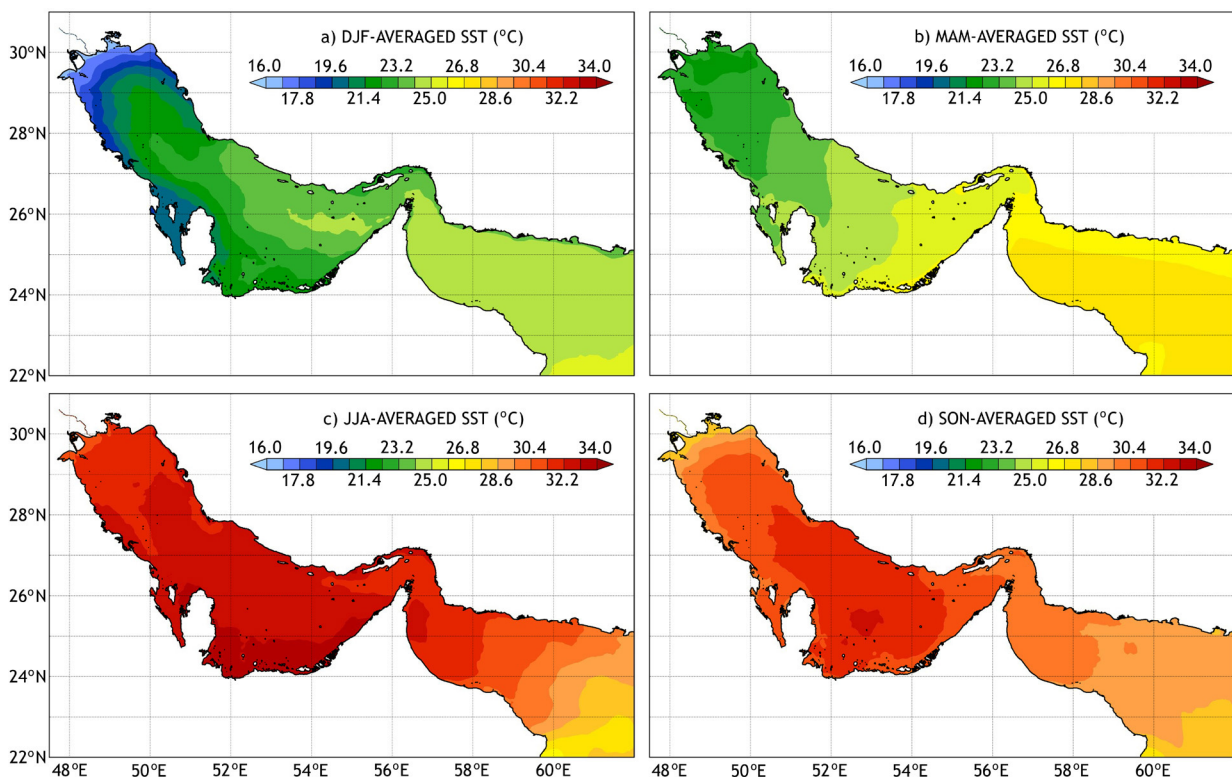

Figure 8 Seasonal mean SSTs averaged over the (a) DJF, (b) MAM, (c) JJA, and (d) SON seasons.
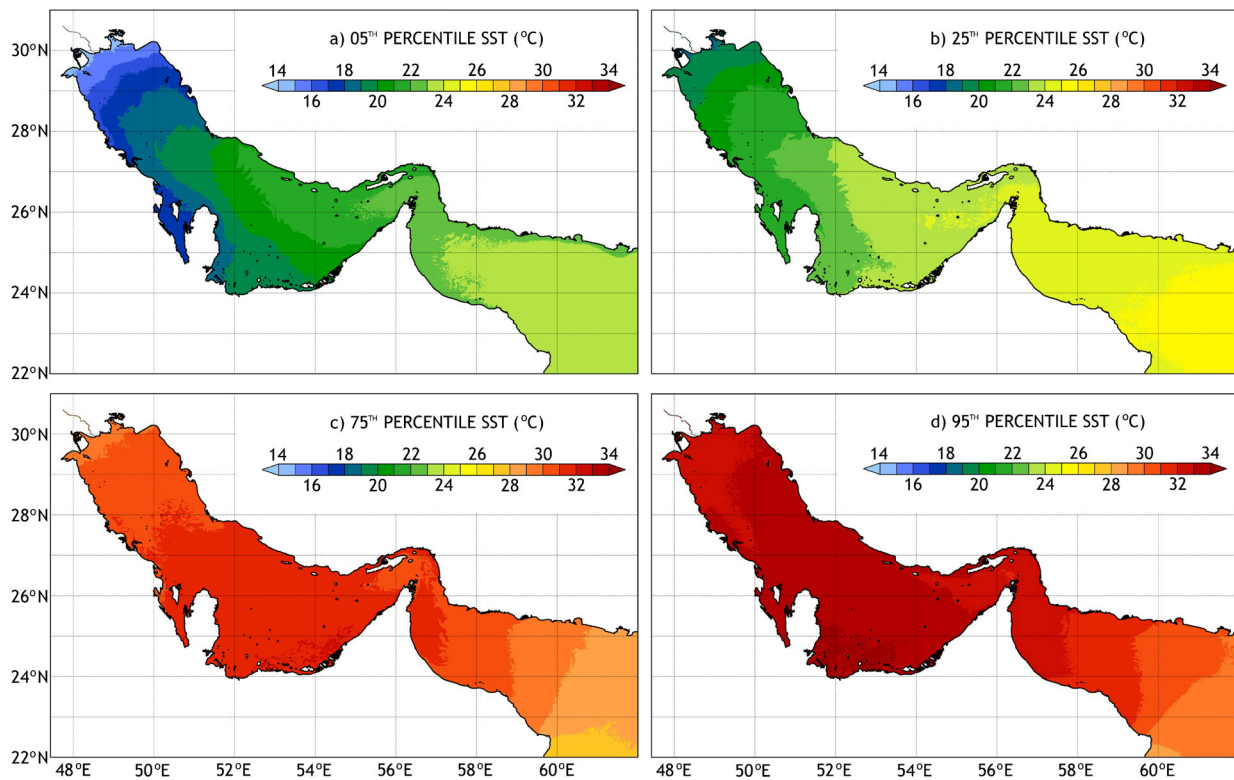
Figure 9   (a) 5th (P_{05}), (b) 25th (P_{25}), (c) 75th (P_{75}), and (d) 95th (P_{95}) percentile SSTs.

generally positive west—east gradients of the P_{05} and P_{25} and the generally negative west—east gradients of the P_{75} and P_{95} SST statistics are found similar to those observed in the winter—spring and summer—autumn seasonal mean SSTs, respectively. Interestingly, the existence of the zone of locally decreased P_{75} and P_{95} SSTs in the Strait of Hormuz is evident in Figures 9c and 9d, similarly to the existence of the zone of local decreases of the annual mean SST (Figure 6a).

3.5. Time exceedances

In addition to the SST percentiles discussed in the Section 3.4, estimating the fractions of the time the SSTs exceed selected temperature levels may also be important. Figure 10 shows the percentages of time, when the SSTs exceeded the temperature levels of 24, 27, 30, and 33°C based on GHRSST data. Generally, a choice of these levels is problem-specific, and it is associated with engineering design criteria or biological tolerance limits.

The SSTs exceeded 24°C more than 80% of the time in the central Gulf and approximately half of the time in the Sea of Oman and the northwestern Gulf. The pronounced west—east gradient, however, vanishes for the temperature level of 27°C, with the highest time exceedances of 60—70% occurring along the UAE and northern Oman coastlines and the lowest time exceedances of 35—45% occurring in the extreme northwestern Gulf and the eastern Sea of Oman. The smaller SST range in the Arabian Sea compared to that in the northwestern half of the Arabian Gulf (Figure 6b) leads to

lower percentages of the time when the SSTs exceed 27°C, despite the higher annual means.

The results for the temperature level of 30°C exhibited a similar spatial pattern to that of 27°C, but at lower percentages ranging from less than 5% in the Arabian Sea to approximately 45% in the southern Gulf and northwestern Sea of Oman. SSTs exceeding 33°C occurred less than 20% of the time in most of the Gulf, except in the western UAE and eastern Qatar waters. Despite the extremely hot summer conditions in the northernmost Gulf (Al Sarmi and Washington, 2014), SSTs exceeding 33°C occurred there less than 5% of the time. In 95% of the time, the SSTs in the Gulf east of Ajman and in the Sea of Oman were lower than 33°C.

3.6. Long-term trends

The mean SST trend for the 17-year study period is presented in Figure 11a. The trend was between 0.02 and 0.04°C/year in most of the Gulf, with a maximum rate of approximately 0.08°C/year in the northern areas between Kuwait City and Bushehr. The estimated trend magnitudes are consistent with those reported in the previous studies: 0.05 ±0.03°C/year in the northern Gulf according to Al-Rashidi et al. (2009); 0.003—0.04°C/year and 0.0005—0.05°C/year in the southern and northern Gulf, respectively, per Shirvani et al. (2015); and 0.03°C/year according to Noori et al. (2019). In particular, Noori et al. (2019) forecasted a 4.3°C increase over the Gulf by August 2100 with respect to 2015 and minimal changes in the Sea of Oman. The smaller rates of the SST changes in the Sea of Oman are in line with the commonly accepted fact that the wa-
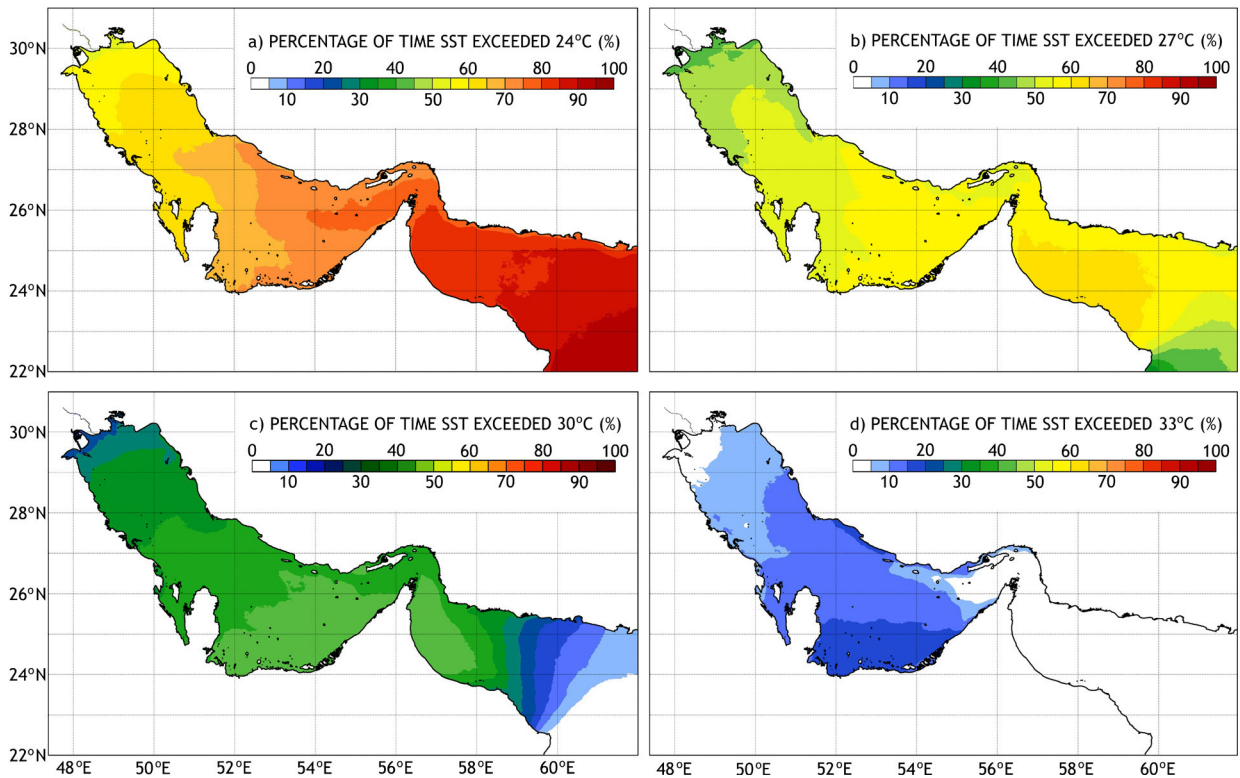
Figure 10 Percentage of the time the SSTs exceeded: (a) 24°C, (b) 27°C, (c) 30°C, and (d) 33°C.

ter and air temperatures in the tropics are significantly less affected by climate change than those in higher latitude regions (e.g., Savo et al., 2016; Seidel et al., 2008). In the Sea of Oman, the RMSE of the linear fit was found comparable to the magnitude of the temperature change over the studied period (see Figure 11b; the 0.02°C/year rate is equivalent to 0.34°C for the 17-year period, close to the RMSE value of approximately 0.3°C). However, in the northwestern part of the Gulf the later was found to be more than three times larger than the former. To determine regions where the obtained trends are statistically significant, a p-value test was conducted. The stippling in Figure 11a indicates the area where the p-value, estimated using a two-tailed t-distribution, did not exceed the 0.05 significance level. Interestingly, the orientation of the elongated footprint of the largest mean SST trends in the northwestern and central Gulf is aligned with the prevailing wind direction (Figure A.1), which suggests that the effect of the mean SST raise in the Gulf is likely associated with the characteristics of air masses coming from the northwest.

In addition to the mean trends, the inter-annual trends in the annual exceedance statistics were also analyzed for a better understanding of the ongoing changes in the extreme SSTs. Figures 11c, 11d, 11e and 11f show the trends in the 5th (P_{05}) and 95th (P_{95}) percentile SSTs, and the RMSEs associated with corresponding linear fits. To derive these trends, the P_{05} and P_{95} percentiles were first calculated for each individual year of the analyzed 17-year period. Then linear fits of 17 samples at each gridded location were obtained and supplemented by a p-value test. Similar to the stippling in Figure 11a, the stippling in resultant Figures 11c and 11e

indicates areas where the p-value, estimated using a two-tailed t-distribution, did not exceed the significance level of 0.05.

As seen in Figure 11c, the occurrence of extreme cold SST events has become more frequent across most of the Gulf, particularly in the shallow regions around Qatar, the western UAE, and the upper northwestern parts of the Gulf. This suggests a recent increase in the frequency of occurrence and magnitude of so-called "cold waves" in the Gulf region, consistent with Almazroui et al. (2014), who found that the "cold waves" in Saudi Arabia have become more extreme compared to those of previous decades, despite the significant overall warming trend. However, the RMSEs associated with the P_{05} trend estimation in the western UAE and eastern Qatar waters were approximately 1°C, which led to the conclusion that the obtained negative trends are statistically insignificant at 95% confidence level in most of the Gulf, possibly reflecting a large variability of the winter lows.

The most pronounced trends in the P_{95} SSTs were found at approximately 0.1°C/year, and they occurred in the western UAE and eastern Qatar waters, the same areas where the highest SSTs were typically observed (see Figures 9d and Figure 10d). This indicates that the extreme high SST events are becoming more frequent and more extreme, regardless of the climatological means. The respective RMSEs in this area were found less than 0.5°C (derived from the fitting over the 17-year period), which makes the obtained results statistically significant with a 95% confidence level. Noteworthy, in some areas of the Sea of Oman, the P_{95} of the SST distribution exhibited decreasing trends with rates up
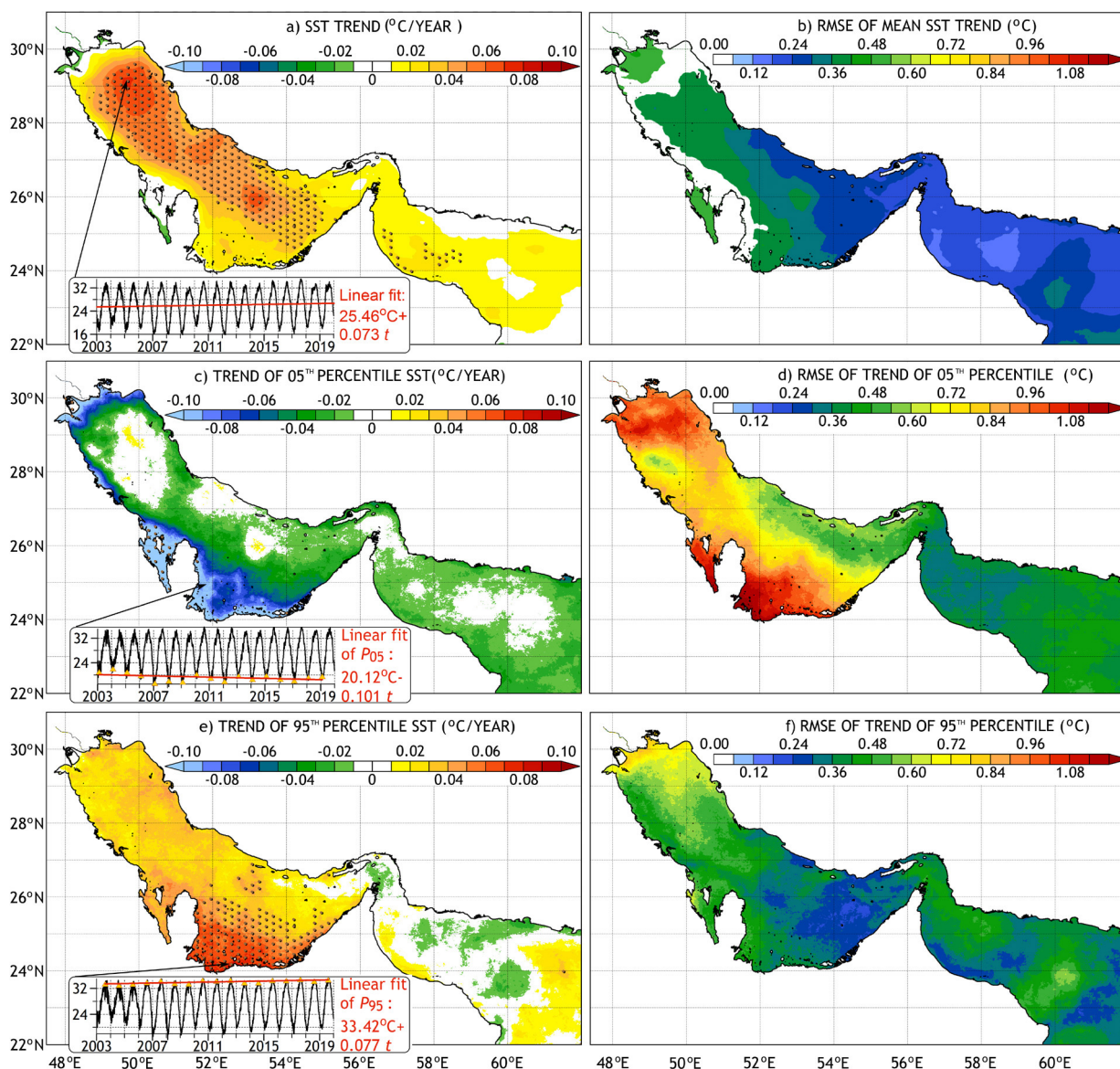
Figure 11 (a, c, e) Trends and (b, d, f) corresponding RMSEs of the mean, annual P_{05}, and annual P_{95} SSTs, respectively. Stippled areas indicate statistical significance at a 95% confidence level. Linear fits at selected locations demonstrating the trends (t is expressed in years starting from 2003) are included as inset plots in panels a, c, and e.

to approximately -0.02°C/year (Figure 11e); however, the RMSEs associated with their respective fits are twice larger than those in the UAE coastal waters in the Gulf.

4. Discussion

An in-depth analysis of the sea surface temperatures in the Arabian Gulf and Sea of Oman was conducted based on GHRSST Level 4 data and in situ seawater temperature measurements. The accuracy of the GHRSST datasets in the Arabian Gulf was evaluated by comparing it with 2-year temperature records obtained from YSI sensors deployed at the ten offshore ADOOS buoys in the UAE coastal waters. The

two datasets were found in a reasonably good agreement, with RMS differences ranging from 0.5 to 1°C, depending on the location, and correlation coefficients exceeding 0.99 for all the ten buoys. After evaluating the accuracy of the GHRSST dataset, a detailed statistical analysis of the SSTs in the Arabian Gulf and Sea of Oman was conducted. The main findings of this study are summarized below.

The highest annual mean SSTs of 28.0°C in the Arabian Gulf and 28.2°C in the Sea of Oman were estimated approximately 80 km northwest of Dubai and along the northwestern shores of Oman between Fujairah and Sohar, respectively. The footprint of the locally elevated SSTs between Fujairah and Sohar in summer correlates with the area of weaker winds, which may possibly explain this effect. The

annual mean temperatures gradually decrease in the Sea of Oman toward the Arabian Sea (27°C near Sur) and toward the Strait of Hormuz (27.5°C). The inter-seasonal SST variabilities were found as large as $\pm 7°C$ with respect to the annual means in the far northwestern part of the Gulf, but they were within the $\pm 1°C$ range in the southeastern part of the Sea of Oman.

The annual maximum SSTs typically occurred in late July to early August in the Sea of Oman, but 2—4 weeks later in the Gulf, except for its shallow near-shore zones. Such a notable difference in timing of the maximum SST occurrences has been attributed to the fact that the daily mean air temperatures remain higher than the SSTs until mid-August, despite they start decreasing in the deserts adjacent to the Gulf after mid-July.

The waters between the western UAE (around Ruwais and Barakah) and eastern Qatar coasts are found to experience the highest SSTs within the studied region during summer, with the 95th percentile SSTs exceeding 34°C. The exceedances of 33°C occurred along the shore between Dubai and Doha 20% of the time, but less than 5% of the time in the northern Gulf, east of Ajman, and the Sea of Oman.

The fluctuations of SST with respect to 24-h running averages at the ADOOS buoy locations were found mostly in the range from -0.8 to 1.4°C (95th percentile deviations), with the magnitudes of the diurnal variabilities typically being less than 2°C (95th percentile range), consistent with the previous studies (e.g., Paparella et al., 2019).

The GHRSST data exhibited mean SST trends mostly in the range from 0.02 to 0.04°C/year, with a maximum of 0.08°C/year in the northern Gulf between Kuwait City and Bushehr, also consistent with the previously reported estimates (e.g., Al-Rashidi et al., 2009; Noori et al., 2019; Shirvani et al., 2015). In addition to the mean SST trends, the inter-annual trends in the annual P_{95} and P_{05} percentile SSTs were analyzed. A rather pronounced trends of annual P_{95} up to 0.07°C/year were estimated in the western UAE and eastern Qatar waters, an area different from that where the highest mean trends were found. These estimations were determined statistically significant with a 95% confidence level. Similarly, cold extremes in the shallow areas around Qatar also exhibited a rather pronounced negative trend of up to $-0.1°C/year$ of the annual P_{05} statistics. This indicates that the extreme hot and cold SST events are becoming more frequent and more extreme in the western UAE and eastern Qatar waters, similarly as it occurs for the trends of extreme air temperatures in the Gulf region (Al Sarmi and Washington, 2014).

Further studies are necessary to explain several interesting peculiarities in the computed SST statistics, namely:

1. The gradual increase in the magnitudes of diurnal SST fluctuations with respect to the daily means from east to west. The P_{50} (median) and P_{99} of the diurnal ranges at Buoy No. 1 located near Dubai were at 0.7 and 1.8°C, respectively, while in the western UAE at Buoy No. 10, they were at 0.8 and 3.3°C, respectively. No apparent correlation with depth or current that could explain this effect was identified; a possible explanation could be association with the effect of sea breezes, which are weaker in the western UAE.

2. The spatial shift of the peak SSTs in the Gulf off the coast to an area approximately 130 km east of Doha and 130 km north of Ruwais during transition from the summer to autumn season. Presumably, this could be attributed to the larger heat capacity of the deeper water column, and higher offshore air humidity in this area, which reduces the rate of radiative cooling of the water surface during autumn.

3. The localized decrease in the annual mean, 75th and 95th percentile SSTs in the Strait of Hormuz near Khasab, where these quantities were up to 1°C lower than in the adjacent regions of the Gulf and Sea of Oman. This decrease is most pronounced in July—September, coinciding with locally increased wind speeds in this season, which may possibly explain this effect. Another possible explanation is that it is caused by more intense vertical mixing due to stronger currents, or due to the surfacing of colder waters in areas with steep bathymetric changes.

Favoring a high spatial resolution of the GHRSST Level 4 dataset, which helped to identify several spatiotemporal features of the SST in the study area, this study was, however, limited by the period of available data, which precluded a more reliable analysis of the SST variability on an inter-decadal scale, and the impact of such phenomena as El Niño oscillation. Another limitation is that the GHRSST data cannot be utilized to investigate diurnal fluctuation of the SSTs. Finally, a spatial resolution of 0.01° × 0.01° is still insufficient to analyze the impacts of individual hot water outfalls in coastal areas.

Acknowledgments

Appendix A. Supporting wind data and statistics at selected locations

A.1. Monthly averaged wind patterns

The monthly averaged horizontal wind plots, which are used to support discussions in this study, are presented in Figure A1.
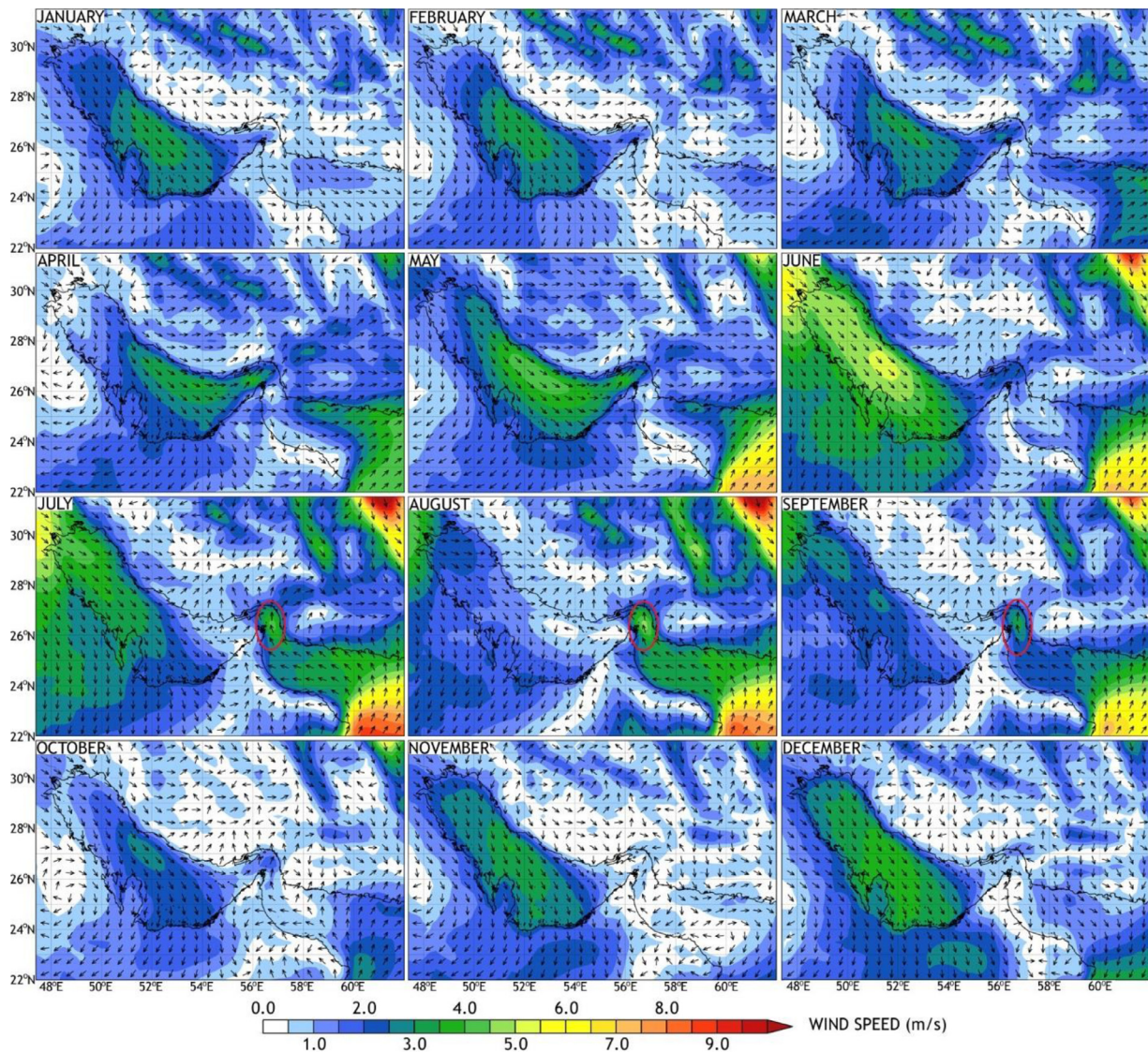
Figure A.1 Monthly averaged horizontal wind over the 2003—2019 period sourced from ERA-5 reanalysis data at 10 m elevation. The shading and arrows represent the speed and direction of the wind, respectively. Red circles denote the locally stronger winds in the Strait of Hormuz in late summer.

A.2. Statistical comparison of ADOOS and GHRSST data

A comparison of 5th (P_{05}) and 95th (P_{95}) percentile SSTs based on in situ ADOOS buoy data against GHRSST data for each season and the RMSDs of daily averaged ADOOS data from the GHRSST data, are presented in Table A1. The comparison was performed for the 2018—2019 period, when in situ data were made available for this study.

A.3. Statistical characteristics of SST at selected locations

The statistical characteristics of the SSTs extracted at several selected coastal locations, such as major cities and industrial sites along the Arabian Gulf and Sea of Oman shores, are summarized in Table A2. For convenience, the sites are listed in counterclockwise order around the Gulf (these locations are indicated in Figure 1).

Table A.1 Comparison of the 5th and 95th percentile SSTs derived from the in situ ADOOS buoy data and GHRSST data extracted at the ten buoy locations covering the 2018—2019 period, and the RMSDs (R) between the daily averaged ADOOS buoy and GHRSST data for each season.

Buoy No.	Spring (°C)							Summer (°C)							Autumn (°C)							Winter (°C)						
	P_{05}		P_{95}		R			P_{05}		P_{95}		R			P_{05}		P_{95}		R			P_{05}		P_{95}		R		
	ADOOS	GHRSST	ADOOS	GHRSST				ADOOS	GHRSST	ADOOS	GHRSST				ADOOS	GHRSST	ADOOS	GHRSST				ADOOS	GHRSST	ADOOS	GHRSST			
1	22.8	21.7	31.2	31.0	0.90			32.4	31.8	35.5	35.0	0.82			25.5	26.2	33.7	33.3	0.49			19.6	19.9	25.1	25.1	0.46		
2	23.3	21.3	31.1	30.5	0.58			31.6	31.4	35.1	34.8	0.61			27.0	26.9	34.3	33.5	0.40			20.6	20.3	26.3	26.0	0.41		
3	21.9	21.6	31.9	31.1	0.97			32.5	31.9	35.6	35.1	0.83			25.5	26.1	33.9	33.4	0.45			19.9	19.4	25.0	24.8	0.40		
4	21.6	21.4	30.8	30.6	0.57			32.0	31.3	35.3	34.9	0.76			26.8	26.8	34.4	33.8	0.80			20.1	20.0	26.0	25.9	0.38		
5	22.4	21.6	31.6	31.3	0.86			32.0	31.9	35.6	35.0	0.83			25.2	25.7	33.9	33.5	0.39			19.5	19.2	24.8	24.6	0.39		
6	21.3	21.0	31.0	30.7	0.60			31.8	31.3	35.5	35.0	0.77			26.2	26.2	34.3	33.6	0.43			19.8	19.6	25.3	25.2	0.39		
7	21.7	21.4	31.4	31.1	0.70			31.9	31.5	35.7	35.1	0.77			25.6	25.4	34.3	34.0	0.44			19.3	19.0	25.1	24.9	0.36		
8	21.6	20.8	31.4	30.7	1.13			31.8	30.9	35.8	35.3	0.79			-*	25.8	-*	34.6	0.40			19.3	19.0	23.8	24.9	0.49		
9	20.1	20.3	31.0	30.4	0.56			31.5	31.1	35.5	35.1	0.71			26.5	26.2	34.7	34.5	0.38			18.9	18.3	25.2	25.1	0.46		
10	19.6	19.9	30.8	30.1	0.60			30.8	30.8	34.6	35.2	0.87			-*	25.9	-*	34.7	1.42			18.8	18.4	23.6	24.8	0.49		

* Prolonged intervals of missing data at buoys Nos. 8 and 10 during the second halves of both autumn seasons corrupt statistical quantities, especially P_{05}, and hence they are not presented in this table.

Table A.2 Statistical characteristics of SST at selected locations based on the GHRSST data 2003—2019.

Location	Coordinates		Seasonal means (°C)					Exceedance (°C)			Trend (°C/year)
	Lon. (°E)	Lat. (°N)	DJF	MAM	JJA	SON	Mean	P_{05}	P_{50}	P_{95}	
Sur	59.54	22.58	24.3	26.9	28.7	28.5	27.1	23.3	27.5	30.5	0.015
Muscat	58.56	23.66	24.2	27.1	30.6	29.2	27.8	23.1	28.6	31.7	0.009
Sohar	56.80	24.36	23.9	27.4	31.7	29.7	28.2	22.8	29.2	32.6	0.016
Fujairah	56.41	25.11	23.9	26.7	32.0	29.9	28.2	22.8	28.9	32.8	0.015
Dibba	56.29	25.61	23.7	26.3	31.9	29.7	27.9	22.6	28.5	32.6	0.015
Khasab	56.26	26.25	23.6	25.5	31.6	29.9	27.7	22.2	28.1	32.5	0.013
Ras Al Khaimah	55.94	25.82	23.4	25.9	32.3	30.4	28.0	22.0	28.6	33.3	0.022
Ajman	55.42	25.44	22.9	25.8	32.5	30.5	28.0	21.3	28.7	33.5	0.025
Dubai	55.20	25.30	22.9	25.6	32.5	30.7	28.0	21.2	28.8	33.5	0.025
Abu Dhabi	54.32	24.53	22.0	26.0	32.8	30.6	27.9	20.2	28.9	34.0	0.025
Ruwais	52.72	24.21	21.9	25.5	32.7	30.9	27.8	19.9	28.6	34.4	0.028
Barakah	52.21	24.01	21.6	25.3	32.7	30.6	27.6	19.5	28.5	34.2	0.014
Doha	51.62	25.33	20.7	24.8	32.5	30.1	27.1	18.6	27.9	34.4	0.007
Manama	50.72	26.28	20.1	24.1	32.3	29.9	26.7	18.2	27.4	34.2	0.007
Al Jubail	49.78	27.08	20.8	23.0	31.7	30.1	26.4	18.6	27.1	33.5	0.031
Khafji	48.66	28.44	19.3	22.3	31.5	29.4	25.7	17.1	26.4	33.2	0.030
Kuwait City	48.04	29.45	17.5	22.4	30.7	28.0	24.7	15.1	25.7	32.7	-0.004
Faw	48.39	29.87	17.1	22.1	30.5	27.7	24.4	14.8	25.4	32.4	-0.019
Deylam	50.08	30.04	18.0	22.5	31.4	28.6	25.2	15.9	25.9	33.4	0.014
Bushehr	50.73	28.88	20.3	22.9	31.4	29.9	26.2	18.1	26.7	33.8	0.050
Kish	54.06	26.55	23.2	24.9	31.8	30.7	27.7	21.6	28.2	33.2	0.026

References

Aeby, G.S., Howells, E., Work, T., Abrego, D., Williams, G.J., Wedding, L.M., Jamie, M., Caldwell, J.M., Moritsch, M., Burt, J.A., 2020. Localized outbreaks of coral disease on Arabian reefs are linked to extreme temperatures and environmental stressors. Coral Reefs 39, 829—846. https://doi.org/10.1007/s00338-020-01928-4

Ahmad, F., Sultan, S.A.R., 1990. Annual mean surface heat fluxes in the Arabian Gulf and the net heat transport through the Strait of Hormuz. Atmosphere-Ocean 29, 54—61. https://doi.org/10.1080/07055900.1991.9649392

Almazroui, M., Islam, M.N., Dambul, R., Jones, P.D., 2014. Trends of temperature extremes in Saudi Arabia. Int. J. Climatol. 34, 808—826. https://doi.org/10.1002/joc.3722

Azam, M.H., Elshorbagy, W., Nakata, K., 2006. Threedimensional modeling of the Ruwais coastal area. J. Waterw. Port C.-ASCE 132 (6), 487—495. https://doi.org/10.1061/(ASCE)0733-950X(2006)132:6(487)

Al Azhar, M., Temimi, M., Zhao, J., Ghedira, H., 2016. Modeling of circulation in the Arabian Gulf and the Sea of Oman: Skill assessment and seasonal thermohaline structure. J. Geophys. Res.-Oceans 121, 1700—1720. https://doi.org/10.1002/2015JC011038

Al Sarmi, S.H., Washington, R., 2014. Changes in climate extremes in the Arabian Peninsula: analysis of daily data. Int. J. Climatol. 34, 1329—1345. https://doi.org/10.1002/joc.3772

Al-Rashidi, T.B., El-Gamily, H.I., Amos, C.L., Rakha, K.A., 2009. Sea surface temperature trends in Kuwait Bay. Arabian Gulf. Nat. Hazards 50, 73—82. https://doi.org/10.1007/s11069-008-9320-9

Al Senafi, F., Anis, A., 2015. Shamals and climate variability in the Northern Arabian/Persian Gulf from 1973 to 2012. Int. J. Climatol. 35, 4509—4528. https://doi.org/10.1002/joc.4302

Banzon, V., Smith, T.M., Chin, T.M., Liu, C., Hankins, W., 2016. A long-term record of blended satellite and in situ sea-surface temperature for climate monitoring, modeling and environmental studies. Earth Syst. Sci. Data 8, 165—176. https://doi.org/10.5194/essd-8-165-2016

Bath, A., Shackleton, B., Botica, C., 2004. Development of temperature criteria for marine discharge from a large industrial seawater supplies project in Western Australia. In: Proc. of the 2004 Water Institute of Southern Africa (WISA) Biennial Conference, 2-6 May 2004, Cape Town, South Africa, 30, Water S.A., 589—599.

Bogdanoff, A.S., Westphal, D.L., Campbell, J.R., Cummings, J.A., Hyer, E.J., Reid, J.S., Clayson, C.A., 2015. Sensitivity of infrared sea surface temperature retrievals to the vertical distribution of airborne dust aerosol. Remote Sens. Environ. 159, 1—13. https://doi.org/10.1016/j.rse.2014.12.002

Chandy, J.V., Coles, S.L., Abozed, A.I., 1990. Seasonal cycles of temperature, salinity and water masses of the western Arabian Gulf. Oceanol. Acta 13, 273—281.

Chowdhury, S., Al-Zahrani, M., 2013. Implications of climate change on water resources in Saudi Arabia. Arab J. Sci. Eng. 38, 1959—1971. https://doi.org/10.1007/s13369-013-0565-6

Claereboudt, M., 2009. Need for actual sea surface temperature data: case study from coral bleaching and remotely sensed "Degree Heating Weeks". Workshop on Marine Monitoring Buoys. Middle East Desalination Research Center, Muscat, the Sultanate of Oman 28 April 2009.

Dubach, H.W., 1964. A summary of temperature-salinity characteristics of the Persian Gulf. National Oceanographic Data Center, General Series, Publ. G-4, 223 pp. https://doi.org/10.5962/bhl.title.39111

Eager, R.E., Raman, S., Wootten, A., Westphal, D.L., Reid, J.S., Al Mandoos, A., 2008. A climatological study of the sea and land breezes in the Arabian Gulf region. J. Geophys. Res. — Atmos 113, D15106. https://doi.org/10.1029/2007JD009710

Elhakeem, A., Elshorbagy, W., Bleninger, T., 2015. Long-term hydrodynamic modelling of the Arabian Gulf. Mar. Pollut. Bull. 94 (1—2), 19—36. https://doi.org/10.1016/j.marpolbul.2015.03.020

Elshorbagy, W., Azam, M.H., Taguchi, K., 2006. Hydrodynamic characterization and modeling of the Arabian Gulf. J. Waterw. Port C.-ASCE 132 (1). https://doi.org/10.1061/(ASCE)0733-950X(2006)132:1(47)

Elshorbagy, W., Azam, M.H., Al Hakeem, A.A., 2013. Temperature-salinity modelling for Ruwais Coast, United Arab Emirates. Mar. Pollut. Bull. 73, 170—182. https://doi.org/10.1016/j.marpolbul.2013.05.025

Environmental Research and Wildlife Development Agency (ER-WDA), Abu Dhabi, UAE, 1999. Federal Environmental Law 24/1999. Technical Guidance Document Standards and Limits for: Pollution to Air and Marine Environment. Occupational Exposure; Pesticides and Chemical Use.

Hersbach, H., Bell, B., Berrisford, P., Dahlgren, P., Horanyi, A., Munoz-Sebater, J., Nicolas, J., Radu, R., Schepers, D., Simmons, A., Soci, C. , 2020. The ERA5 Global Reanalysis: achieving a detailed record of the climate and weather for the past 70 years. European Geophysical Union General Assembly 2020, May 38, Vienna, Austria https://doi.org/10.5194/egusphere-egu2020-10375

Kämpf, J., Sadrinasab, M., 2006. The circulation of the Persian Gulf: a numerical study. Ocean Sci. Dis. 2, 27—41. https://doi.org/10.5194/osd-2-129-2005

Mahto, S.S., Mishra, V., 2019. Does ERA-5 outperform other reanalysis products for hydrologic applications in India? J. Geophys. Res.-Atmos. 124, 9423—9441. https://doi.org/10.1029/2019JD031155

Mezhoud, N., Temimi, M., Zhao, J., Al Shehhi, M.R., Ghedira, H., 2016. Analysis of the spatio-temporal variability of seawater quality in the southeastern Arabian Gulf. Mar. Poll. Bull. 106 (1—2), 127—138. https://doi.org/10.1016/j.marpolbul.2016.03.016

Ministry of Regional Municipalities, Environment and Water Resources, the Sultanate of Oman, 2005. Ministerial Decision No. 159/2005. Promulgating the Bylaws to Discharge Liquid Waste into the Marine Environment.

Minnett, P., Kaiser-Weiss, A., 2012. Discussion document: Near-surface oceanic temperature gradients, Version 12 Jan 2012. Available at www.ghrsst.org. Last Access: 31 January 2021.

Moradi, M., Kabiri, K., 2015. Spatio-temporal variability of SST and chlorophyll-a from MODIS data in the Persian Gulf. Mar. Poll. Bull. 98, 14—25. https://doi.org/10.1016/j.marpolbul.2015.07.018

Nesterov, O., Scraggs, C., Smit, F., Mocke, G.P., 2010. Modelling of hydrodynamics and seawater temperature along the UAE Coast. In: Proc. Second International Conference on Coastal Zone Engineering and Management (Arabian Coast 2010). Muscat, Oman 1—3 November 2010.

Noori, R., Tian, F., Berndtsson, R., Abbasi, M.R., Naseh, M.V., Modabberi, A., Soltani, A., Kløve, B., 2019. Recent and future trends in sea surface temperature across the Persian Gulf and Gulf of Oman. PLOS ONE 14 (2), e0212790. https://doi.org/10.1371/journal.pone.0212790

Paparella, F., Xu, X., Vaughan, G.O., Burt, J.A., 2019. Coral bleaching in the Persian/Arabian Gulf is modulated by summer winds, Front. Mar. Sci. 6, 205. https://doi.org/10.3389/fmars.2019.00205

Pastor, F., Valiente, J.A., Palau, J.L., 2018. Sea surface temperature in the Mediterranean: trends and spatial patterns (1982—2016). Pure Appl. Geophys 175, 4017—4029. https://doi.org/10.1007/s00024-017-1739-z

Pous, S.P., Carton, X., Lazure, P., 2004. Hydrology and circulation in the Strait of Hormuz and the Gulf of Oman — Results from the GOGP99 Experiment. J. Geophys. Res. — Oceans 109. https://doi.org/10.1029/2003JC002146

Pous, S., Lazure, P., Carton, X., 2015. A model of the general circulation in the Arabian Gulf and in the Strait of Hormuz: Intraseasonal to interannual variability. Cont. Shelf Res. 94, 55—70. https://doi.org/10.1016/j.csr.2014.12.008

Qasim, S.Z., 1982. Oceanography of the northern Arabian Sea. Deep-Sea Res 29, 1041—1068. https://doi.org/10.1016/0198-0149(82)90027-9

Reul, N., Chapron, B., Lee, T., Donlon, C., Boutin, J., Alory, G., 2014. Sea surface salinity structure of the meandering Gulf Stream revealed by SMOS sensor. Geophys. Res. Lett. 41 (9), 3141—3148. https://doi.org/10.1002/2014GL059215

Reynolds, R.M., 1993. Physical oceanography of the Gulf, Strait of Hormuz, and the Gulf of Oman—Results from the Mt Mitchell expedition. Mar. Pollut. Bull. 27, 35—59. https://doi.org/10.1016/0025-326X(93)90007-7

Royal Commission for Jubail and Yanbu, Environmental Control Department, the Kingdom of Saudi Arabia, 2004. Royal Commission Environmental Regulation.

Savo, V., Lepofsky, D., Benner, J.P., Kohfeld, K.E., Kohfeld, K.E., Bailey, J., Lertzman, K., 2016. Observations of climate change among subsistence-oriented communities around the world. Nat. Clim. Change 6, 462—473. https://doi.org/10.1038/nclimate2958

Seidel, D.J., Fu, Q., Randel, W.J., Reichler, T.J., 2008. Widening of the tropical belt in a changing climate. Nat. Geosci. 1, 21—24. https://doi.org/10.1038/ngeo.2007.38

Sheppard, C., Al-Husiani, M., Al-Jamali, F., Al-Yamani, F., Baldwin, R., Bishop, J., Benzoni, F., Dutrieux, E., Dulvy, N.K., Durvasula, R.S.V., Jones, D.A, Loughland, R., Medio, D., Nithyanandan, M., Pilling, G.M, Polikarpov, I., Price, A.R.G., Purkis, S., Riegl, B., Saburova, M., Namin, K.S., Taylor, O., Wilson, S., Zainal, K., 2010. The Gulf: A young sea in decline. Mar. Poll. Bull. 13—38. https://doi.org/10.1016/j.marpolbul.2009.10.017

Shirvani, A., Nazemosadat, S.M.J., Kahya, E., 2015. Analysis of the Persian Gulf sea surface temperature: prediction and detection of climate change signals. Arab J. Geosci. 8, 2121—2130. https://doi.org/10.1007/s12517-014-1278-1

Supreme Council for the Environment and Natural Reserves, the State of Qatar, 2002. Executive By-Law for the Environment Protection Law, the Decree Law No. 30 for the Year 2002.

Swift, S.A., Bower, A.S., 2003. Formation and circulation of dense water in the Persian/Arabian Gulf. J. Geophys. Res. — Oceans 108 (1). https://doi.org/10.1029/2002JC001360

Tahir, Z.R., Azhar, M., Mumtaz, M., Asim, M., Moeenuddin, G., Sharif, H., Hassan, S., 2020. Evaluation of the reanalysis surface solar radiation from NCEP, ECMWF, NASA, and JMA using surface observations for Balochistan, Pakistan. J. Renew Sustain. Ener. 12, 023703. https://doi.org/10.1063/1.5135381

Xue, P., Eltahir, E.A.B., 2015. Estimation of the heat and water budgets of the Persian (Arabian) Gulf using a regional climate model. J. Climate 28, 5041—5062. https://doi.org/10.1175/JCLI-D-14-00189.1